

## Towards a universal ion source: Glow Flow mass spectrometry

Rhodri N. Owen\* (<https://orcid.org/0000-0002-3109-6653>), Steven L. Kelly (<https://orcid.org/0000-0001-7991-5040>) and A. Gareth Brenton\* ([orcid.org/0000-0003-2600-2082](https://orcid.org/0000-0003-2600-2082))

Institute of Life Science, Swansea University Medical School, Swansea, Wales, United Kingdom SA2 8PP

### Highlights

- Flexible and low-cost dc helium-microplasma source has been developed
- Persistent organic pollutants can be readily identified by microplasma ion source
- Components from complex mixtures can be identified

### Abstract

A helium-microplasma ion source (Glow Flow) has been developed and characterised. It is engineered to be a simple design, of low-cost and can be readily retrofitted to most modern mass spectrometers. Initial assessment of its performance has shown it to be robust, reproducible and of high sensitivity. Glow Flow provides broad non-specific detection of samples from polar through to non-polar chemistries making it of wide utility. A study of persistent organic pollutants, polyaromatic hydrocarbons, low average-molecular-mass polymers (polyethyleneimine, polyethylene glycol, and polypropylene glycol) and a complex mixture of fatty-acid methyl esters by direct sample introduction using a nebulised heated nitrogen flow was conducted. The ability to make quantitative measurement was investigated using methyl stearate and a linear calibration plot gave a  $R^2 = 0.999$  and limit-of-detection of  $\sim 100$  fmol. This design is extremely stable, in operation. Typical ions commonly observed are intense protonated molecule ions, radical molecular ions, hydride abstracted ions, and oxygen adduct ions. At present this system is valuable to apply to small molecule analysis ( $m/z < 1000$ ), and is easily interfaced to gas and liquid chromatography, and likely to be useful for imaging.

**Keywords** ionization, ion source, helium microplasma, mass spectrometry, glow discharge, analytical science

\*Authors to which correspondence should be sent.

## 1. Introduction

Atmospheric pressure glow discharge ionization sources have the potential to generate a number of ionization pathways including Penning ionization, charge transfer and protonation amongst others. Curt Brunnée is claimed to have said that there is “no ideal ion source”, and to our knowledge no single source can analyse samples covering most common chemistries. The ideal characteristics of an ion source would include low limits of detection, broad dynamic range, be impervious to matrix effects, have high ionization efficiency, be stable and reproducible, and provide broad non-specific detection (covering polar and non-polar, small and large molecules), whilst readily allowing elemental formulae assignment and thus the identity of the molecular species present. Furthermore, its design ought to allow easy introduction of samples and interface readily to chromatography, have low-power use, low gas and solvent consumption [1].

Studies of, and the application of gas plasmas have long been associated with mass spectrometry. Indeed J.J. Thomson’s first measurements used a low-pressure glow discharge to produce his “canal rays”. For many decades however, the utility of plasma sources has been overshadowed by the ubiquity of electron ionization (EI), first described by Dempster in 1918 [2]. The significance of plasma sources was never far away, initially low pressure [3,4] and subsequently atmospheric pressure ionisation (API) and ambient desorption ionisation (ADI) sources [5-13]. A review of over forty different variants of ADI sources and methods has been published [14]. One feature of this review is the large number of acronyms associated to each variant and is a growing issue for mass spectrometry nomenclature [15]

Interest in atmospheric pressure glow discharge sources was renewed as they have been shown to many of the characteristics of an ideal sources. However, many of the designs have included a discharge cell making them bulky and require adaptation of the source housing of existing to allow operation. Therefore, a more compact ionisation source design which can be retrofitted to existing mass spectrometers would be beneficial. In this paper we describe a design based on a high-voltage dc helium-microplasma operating at atmospheric pressure which has high stability and high sensitivity.

## 2. Materials and Method

### 2.1. Helium-microplasma design

A schematic (Fig. 1A) and photograph (Fig. 1B) of the helium-microplasma source used in this study is shown in Fig. 1. An electrically insulating polyether ether ketone (PEEK) zero-dead volume union is used as the body of the source. The anode, a stainless-steel probe tip assembly (23.5 mm length, o.d. 640  $\mu\text{m}$ , Waters Crop, Manchester, UK) is attached to one end of the union. A PEEK thumb nut (55067-U, Sigma-Aldrich, Gillingham, UK) was used to connect a helium gas line as the gas inlet side of the union. An electrical connection was used to attach the anode electrode to the mass spectrometer’s internal power supply and was operated in constant current mode (1-35  $\mu\text{A}$ ) and the source housing of the instrument acts as the counter electrode, nominally at 0V. The gas flow rate (0.05-0.5  $\text{L}\cdot\text{min}^{-1}$ ) was regulated by a variable area flow meter (Model MR3A12BVBVN, Key Instruments Corp, Treviso, USA). This Glow Flow source is an engineered

reduction of a larger flowing atmospheric-pressure afterglow design, following the cell design of Heiftje [1] we had previously built and used in our laboratory, Glow Flow is housed in a sealed source environment where the pressure and atmospheric composition can be controlled, unlike an external atmospheric arrangement. The source does however have similarities to others, for example, Graham Cooks' group have been very active in this area [16], but they have largely used radio frequency (RF) discharge, as well as the low temperature dielectric barrier discharge ionization (DBDI). It is not the intention to review this area here and the wide range of ADI devices currently developed [14].

<Figure 1 here>

## 2.2. Chemical Reagents

High purity, anthracene, naphthalene, pyrene, bisphenol A, bisphenol S, 1,4-dioxane, dibenzofuran and 2,8-dibromodibenzofuran were purchased from Tokyo Chemical Industry UK Ltd (Oxford, UK), methyl stearate was purchased from Alfa Aesar (Heysham, UK), dichloromethane and methanol were purchased from Fisher Scientific (Loughborough, UK), and analytical standard C4 - C24 even-carbon saturated fatty-acid methyl esters (FAMES), dodecane, tetradecane, octadecane, polypropylene glycol, polyethylene glycol and polyethyleneimine were purchased from Sigma-Aldrich (Gillingham, UK). High purity helium, Grade CP (N5.0) 99.999% (BOC Gas and Gear, Port Talbot, UK) was used for all experiments.

Samples were dissolved in 1:2 (v/v) dichloromethane and methanol solution before being diluted to a suitable working concentration.

## 2.3. Mass spectrometry

Data was acquired on a Xevo G2-S time-of-flight mass spectrometer (Waters Corp, Wilmslow, UK). The source conditions were as follows: in positive ion mode source cone voltage +10 to +30 V, desolvation gas flow 200 L.h<sup>-1</sup> and temperature of 300 °C, and source temperature 120 °C unless otherwise stated. Data was obtained and processed using MassLynx 4.1 (Waters Corp, Wilmslow, UK) and with the R statistical software package [17].

# 3. Results and Discussion

## 3.1. Characterisation of prototype ion source

The prototype ion source can sustain a glow discharge over a broad range of currents 1-35  $\mu\text{A}$ , gas flow rates from 0.05 to 0.5 L.min<sup>-1</sup>, are typical for a small exit tube diameter and electrode distances from 5 to 40 mm. The ion source was positioned axially to a metal plate that was mechanically connected to earth and acted as the counter electrode. The Xevo instrument's internal power supply was initially set to 10  $\mu\text{A}$  in constant current mode and the readback current was recorded as the electrode distance was increased from 5 mm to 40 mm, in 5 mm increments. At distances from 5 to 15 mm the current remained constant (Fig. 2). Above 20 mm the current reduced until, at 40 mm it was 2.9  $\mu\text{A}$  (40 mm was the limit of travel within the source housing). The change in current is also marked by the shortening of the visible plasma column which initially extends the full distance between the electrodes to a tip at the anode, at electrode distances greater than 15 mm.

Solving Paschen's law (1) for an electrical discharge in helium at atmospheric pressure predicts that at the maximum breakdown-voltage that the instrument's internal power supply can deliver, i.e. 5 kV, is reached at an electrode distance of 13.9 mm, which corresponds closely with the observed data. To sustain a glow discharge at electrode distances greater than 13.9 mm with this ion source, the voltage must remain below its maximum threshold and consequently a reduction in the actual current would be expected or the glow discharge would extinguish.

$$V_b = \frac{B \cdot pd}{C + \ln(pd)} \quad (1)$$

where  $V_b$  is the breakdown voltage,  $pd$  is the product of the pressure and inter-electrode distance and  $B$  and  $C$  are constants.

<Figure 2 here>

To ascertain the nature of the glow discharge regime that the helium-microplasma operates under, the output voltage of the system was recorded at different electrode to tip distances and gas flow rates (Fig. 3). At electrode distances of 5 mm the voltage increasing linearly from 274 V at 5  $\mu\text{A}$  to 1.9 kV at 35  $\mu\text{A}$  at all flow rates for 0.2  $\text{L}\cdot\text{min}^{-1}$ . At the larger electrode distance of 20 mm the current-voltage relationship is only linear between 5 and 10  $\mu\text{A}$  at 0.3 to 0.5  $\text{L}\cdot\text{min}^{-1}$ , above which the voltage plateaux. We propose that this change is as a result of a transition between the abnormal glow regime at short electrode distances (0-15 mm), where the voltage increases with current, and is typical for the flowing atmospheric-pressure afterglow (FAPA [18]) ion source, and the normal glow regime, where the voltage is constant with varying current, at larger electrode distances (>20 mm).

<Figure 3 here>

### 3.2. Figures of merit

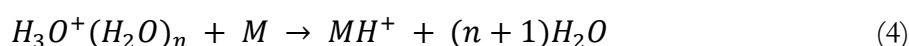
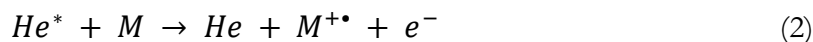
An experiment to determine the reproducibility and sensitivity of the helium-microplasma ion source (Glow Flow) was conducted. Methyl stearate was prepared at concentrations from 5 to 40  $\text{pg}\cdot\mu\text{L}^{-1}$  and one microliter was syringed on to the end of a glass capillary and allowed to dry in air. The glass capillary was introduced into the mass spectrometer source housing by means of an atmospheric-pressure solids analysis probe (ASAP [19]) and the peak area of the  $m/z$  299.29 ion was recorded in full scan mode. This probe does not have an internal heater to desorb the sample and relies on a heated desolvation gas flow (ambient to 650°C) for sample desorption. Based on these findings we estimate the lower limit-of-detection (LOD) to be 111 fmol (Fig. 3). The source also exhibited high sampling reproducibility and a low standard error of the mean at the LOD.

<Figure 4 here>

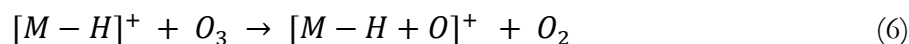
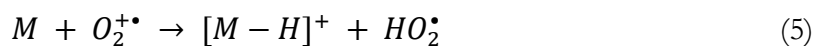
### 3.3. Detection of xenobiotic compounds

Persistent organic pollutants and their analogues have a broad range of chemistries, from apolar (hydrocarbons, halogenated hydrocarbons) to polar (bisphenol). A range of samples were prepared at concentrations of 1  $\mu\text{g}\cdot\mu\text{L}^{-1}$ , with 1  $\mu\text{L}$  syringed onto a glass capillary and allowed to

dry before being introduced into the mass spectrometer source using the probe. The mass spectra were collected using full scan mode and the most intense peaks recorded (Table 1). A range of ions were observed, those more polar compounds tended to produce protonated  $[M+H]^+$  molecules while those apolar compounds tended to produce radical molecular ions  $M^{+\bullet}$ . There are however many instances where molecular ions and protonated molecules are observed in relatively equal intensities, supporting the hypothesis that helium-microplasma like many other plasma ion sources can access multiple ionization pathways including Penning ionization (2), charge transfer (3), and protonation (3).



In particular, a trend is observed in polyaromatic hydrocarbons (PAH) with an increase in intensity of the protonated molecule  $[M+H]^+$ , with increasing proton affinity and a corresponding decrease in the molecular ion  $M^{+\bullet}$  intensity, suggesting that the sample chemistry can be used to determine the most favourable ionization pathway and potentially the ability to tune the source to selectively ionize. The base peak for the straight-chain saturated hydrocarbons was  $M+15$  suggesting the hydrogen atom displacement by oxygen occurs readily for this class of compounds, following reactions (5) and (6) as a possible mechanism which others have proposed [20]. Similarly, we observed phenoxide ion formation in the PAH compounds by displacement of a hydrogen atom in the aromatic ring [21].



An experiment was also conducted in negative ion mode to establish the helium-microplasma ion source's capabilities (Supplementary Information Table S1) with a selected range of compounds. Generally deprotonated ions  $[M-H]^-$  were observed however for the polyaromatic hydrocarbons the oxygen  $[M+O-H]^-$  adduct was observed as the base peak with a weaker signal for the deprotonated ion.

<Table 1 here>

### 3.4. Low molecular weight polymers

Three low average-molecular-mass polymers, polyethyleneimine, polyethylene glycol, and polypropylene glycol, which are normally analysed by electrospray were selected for analysis to assess the ion source's ability to handle samples over a broader range of molecular weight distributions. Samples were prepared at a concentration of  $1 \mu\text{g}\cdot\mu\text{L}^{-1}$  and introduced by the ASAP probe into the source housing as previously described, the desolvation gas temperature was increased progressively  $500^\circ\text{C}$  to volatilise compounds off the probe. Protonated molecules were observed for all three polymers in positive ion mode and a characteristic mass distribution

envelope with repeating  $m/z$  values corresponding to the repeating unit for each compound was noted (Table 2).

<Table 2 here>

### 3.5. Detection of biochemical mixtures

FAMEs were used, as provided at a concentration of  $1000 \text{ ng}\cdot\mu\text{L}^{-1}$  of each component in hexane,  $1 \mu\text{L}$  was syringed on to the end of a glass capillary and allowed to dry in air. The glass capillary was introduced into the mass spectrometer source housing using the ASAP probe. Desolvation gas temperature was increased from  $50$  to  $350 \text{ }^\circ\text{C}$ , in steps of  $25 \text{ }^\circ\text{C}$ . The long chain and very long chain fatty-acid methyl esters are readily observed varying the temperature gradient of the desolvation gas allowed control of which ions were observed (Table 3). Unfortunately, the short and medium chain fatty-acid methyl esters were not observed at the desorption time profile employed, and we were unable to continue that experimental work using a slower temperature desorption profile, due to the Covid19 lockdown [24]. We believe that the compounds were too volatile and swept away in the fast-flowing gas stream in the early part of the rapid desolvation process. Better control of the initial desolvation gas temperature perhaps has to be tailored for such a mixture, to observe lower molecular weight FAME compounds. In future work we will couple and employ gas chromatography and liquid chromatography for mixture analysis, which is preferable as it leads to reduced ionization competition.

<Table 3 here>

## 4. Conclusion

A low-cost and flexible-format helium-microplasma ion source has been developed and characterised. Earlier designs in our laboratory were based on the standard FAPA source designs involving a gas discharge cell [18]. These were found to be less sensitive and reproducible than the Glow Flow design, as implemented on a Xevo mass spectrometer. We moved our development on to the Glow Flow design in late 2019 and found it more sensitive; laboratory work had to cease in March 2020 due to Covid19 disruption [24], otherwise a more thorough report for this invited paper would have been written.

Initial assessment has shown Glow Flow to have good sampling reproducibility and has high sensitivity for the compounds tested comparable to a GC-FAPA time-of-flight mass spectrometer used for the analysis of dodecane (LOD  $12 \text{ pg}\cdot\mu\text{L}^{-1}$  c.f. [25]). The source has shown the ability to be applied to small molecules and to more complex synthetic polymers. Use of alternative plasma gasses and adjuvants, to enhance ionization sensitivity or molecular species identity, will be investigated and the ion source will be applied to the analysis of biomolecules and its potential for elemental analysis will be investigated. The source could be easily adapted and retrofitted to most atmospheric pressure and ambient desorption ionization instruments in combination with a range of sample inlets. It could also be potentially mounted on a X-Y movable stage to provide spatial data as part of a mass spectrometry imaging platform. A key to Glow Flow's wider application lies in the successful intact evaporation of samples into the microplasma, either by nebulization, indirect heating or direct heating by the plasma (which is a less easy method to precisely control

volatization of small amounts of material). Further work by coupling GC and LC will present samples in the gas phase and nebulized form. Research will focus on how samples are presented, which region of the micro-plasma suits different sample types and the use of adjuvant molecules to enhance ionization as shown in the work of Trimpin [26]. These plasma sources can produce highly intense protonated molecule ions, radical molecular ions, hydride abstracted ions, and oxygen adduct ions are commonly observed. However, a complicating feature found for certain compound classes show ions that have undergone complex chemistry resulting in quite unusual or unexpected ions and further research is required to classify the expected ions for different chemical classes to make these sources more friendly for the chemical analyst to adopt more widely.

### Declaration of competing interest

Gareth Brenton is an Emeritus Professor in Swansea Medical School and a director of AberMS Ltd, a company registered in the England and Wales (UK), and holds an interest in the sale and marketing of this helium-microplasma ion source design described in this article.

### CRedit authorship contribution statement

**Gareth Brenton:** Supervision, conceptualization, writing - review & editing. **Steven L. Kelly:** Supervision. **Rhodri N. Owen:** Investigation, visualization, writing - original draft.

### Acknowledgement

This article was prepared on the invitation of the editors as part of a special issue in the run up to the International Mass Spectrometry Society conference. This work was funded by the Engineering and Physical Sciences Research Council (EP/R51312X/1).

### References

1. J.T. Shelley, G.M. Hieftje, Ambient mass spectrometry: Approaching the chemical analysis of things as they are, *J. Anal. At. Spectrom.* 26 (2011) 2153–2159. <https://doi.org/10.1039/C1JA10158G>.
2. A.J. Dempster, A New Method Of Positive Ray Analysis, *Phys Rev.* 11 (1918) 316.
3. M.S.B. Munson, F.H. Field, Chemical Ionization Mass Spectrometry. I. General Introduction, *J. Am. Chem. Soc.* 88 (1966) 2621–2630. <https://doi.org/10.1021/ja00964a001>.
4. W. Grimm, Eine neue glimmentladungslampe für die optische emissionsspektralanalyse, *Spectrochim. Acta B.* 23 (1968) 443–454. [https://doi.org/10.1016/0584-8547\(68\)80023-0](https://doi.org/10.1016/0584-8547(68)80023-0).
5. H.D. Beckey, Principles of field ionization and field desorption mass spectrometry, 1st ed, Pergamon Press, Oxford [Eng.]; New York, 1977.
6. D.I. Carroll, I. Dzidic, R.N. Stillwell, K.D. Haegele, E.C. Horning, Atmospheric pressure ionization mass spectrometry. Corona discharge ion source for use in a liquid chromatograph-mass spectrometer-computer analytical system, *Anal. Chem.* 47 (1975) 2369–2373. <https://doi.org/10.1021/ac60364a031>.
7. A.L. Gray, Mass-spectrometric analysis of solutions using an atmospheric pressure ion source, *Analyst.* 100 (1975) 289–299. <https://doi.org/10.1039/AN9750000289>.

8. H. Kuwabara, M. Tsuchiya, Liquid Ionization Mass Spectrometry of Involatile Organic Compounds: Use of a Needle Electrode and Matrix, J. Mass Spectrom. Soc. Jpn. 30 (1982) 313–318. <https://doi.org/10.5702/masspec.30.313>.
9. R. Mason, D. Milton, Glow discharge mass spectrometry of some organic compounds, Int. J. Mass Spectrom. 91 (1989) 209–225. [https://doi.org/10.1016/0168-1176\(89\)83010-1](https://doi.org/10.1016/0168-1176(89)83010-1).
10. R.B. Cody, J.A. Laramée, H.D. Durst, Versatile New Ion Source for the Analysis of Materials in Open Air under Ambient Conditions, Anal. Chem. 77 (2005) 2297–2302. <https://doi.org/10.1021/ac050162j>.
11. Z. Takáts, J.M. Wiseman, B. Gologan, R.G. Cooks, Mass Spectrometry Sampling Under Ambient Conditions with Desorption Electrospray Ionization, Science. 306 (2004) 471–473. <https://doi.org/10.1126/science.1104404>.
12. G.A. Harris, A.S. Galhena, F.M. Fernández, Ambient Sampling/Ionization Mass Spectrometry: Applications and Current Trends, Anal. Chem. 83 (2011) 4508–4538. <https://doi.org/10.1021/ac200918u>.
13. A. Albert, J.T. Shelley, C. Engelhard, Plasma-based ambient desorption/ionization mass spectrometry: state-of-the-art in qualitative and quantitative, Anal. Bioanal. Chem. 406 (2014) 6111–6127. <https://doi.org/10.1007/s00216-014-7989-z>.
14. J.T. Shelley, S.P. Badal, C. Engelhard, H. Hayen, Ambient desorption/ionization mass spectrometry: evolution from rapid qualitative screening to accurate quantification tool, Anal. Bioanal. Chem. 410 (2018) 4061–4076. <https://doi.org/10.1007/s00216-018-1023-9>.
15. K.K. Murray, R.K. Boyd, M.N. Eberlin, G.J. Langley, L. Li, Y. Naito, Definitions of terms relating to mass spectrometry (IUPAC Recommendations 2013), Pure Appl. Chem. 85 (2013) 1515–1609. <https://doi.org/10.1351/PAC-REC-06-04-06>.
16. J.D. Harper, N.A. Charipar, C.C. Mulligan, X. Zhang, R.G. Cooks, Z. Ouyang, Low-Temperature Plasma Probe for Ambient Desorption Ionization, Anal. Chem. 80 (2008) 9097–9104. <https://doi.org/10.1021/ac801641a>.
17. R Core Team, R: A language and environment for statistical computing., R Foundation for Statistical Computing, Vienna, Austria., 2019. <https://www.R-project.org/>.
18. F.J. Andrade, W.C. Wetzel, G.C.-Y. Chan, M.R. Webb, G. Gamez, S.J. Ray, G.M. Hieftje, A new, versatile, direct-current helium atmospheric-pressure glow discharge, J. Anal. At. Spectrom. 21 (2006) 1175–1184. <https://doi.org/10.1039/B607544D>.
19. C.N. McEwen, R.G. McKay, B.S. Larsen, Analysis of Solids, Liquids, and Biological Tissues Using Solids Probe Introduction at Atmospheric Pressure on Commercial LC/MS Instruments, Anal. Chem. 77 (2005) 7826–7831. <https://doi.org/10.1021/ac051470k>.
20. D.T. Usmanov, L.C. Chen, K. Hiraoka, H. Wada, H. Nonami, S. Yamabe, Mass spectrometric monitoring of oxidation of aliphatic C6–C8 hydrocarbons and ethanol in low pressure oxygen and air plasmas, J. Mass Spectrom. 51 (2016) 1187–1195. <https://doi.org/10.1002/jms.3890>.
21. K. Merrett, A.B. Young, A.G. Harrison, O<sup>-</sup> chemical ionization mass spectra of fluoroaromatic compounds, J. Mass Spectrom. 28 (1993) 1124–1128. <https://doi.org/10.1002/oms.1210281024>.
22. E.P.L. Hunter, S.G. Lias, Evaluated Gas Phase Basicities and Proton Affinities of Molecules: An Update, J. Phys. Chem. Ref. Data. 27 (2009) 413. <https://doi.org/10.1063/1.556018>.
23. R.C. Weast, ed., CRC handbook of chemistry and physics. A ready-reference book of chemical and physical data, 66th ed, CRC Pr, Boca Raton, 1986.
24. COVID-19 lockdown in the UK started in March 2020 c.f. [https://doi.org/10.1016/S1473-3099\(20\)30200-0](https://doi.org/10.1016/S1473-3099(20)30200-0)
25. C.S. Davies, PhD Thesis, “Development of an Advanced Ionisation Technique for Mass Spectrometry: the Flowing Atmospheric Pressure Afterglow (FAPA) Ionisation Source,” Swansea University, 2018.



26. S. Trimpin, C.A. Lutomski, T.J. El-Baba, D.W. Woodall, C.D. Foley, C.D. Manly, B. Wang, C.-W. Liu, B.M. Harless, R. Kumar, L.F. Imperial, E.D. Inutan, Magic matrices for ionization in mass spectrometry, Int. J. Mass Spectrom. 377 (2015) 532–545. <https://doi.org/10.1016/j.ijms.2014.07.033>.

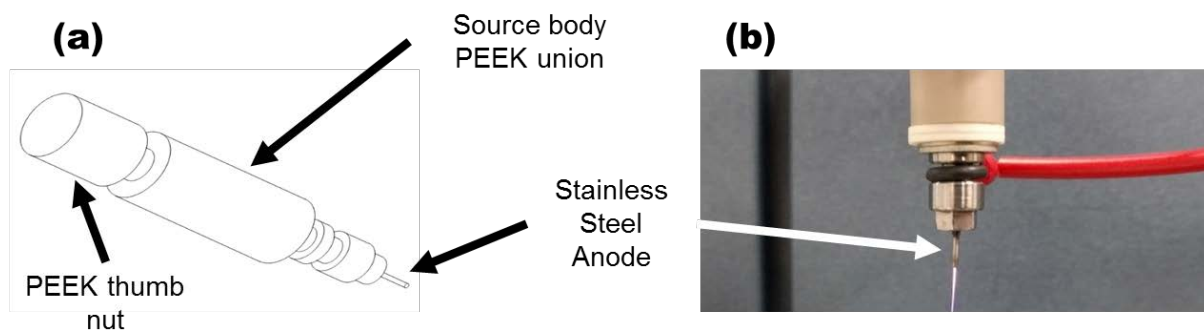


**Fig. 1.** (a) Diagram of the helium-microplasma ion source made up of the PEEK union body and thumb nut (left hand side) and stainless-steel anode connected (right hand side). (b) Photograph of helium-microplasma ion source showing the anode and lower portion of the source body. A high-voltage wire (red) is used for connecting to the instrument internal power supply, the glow discharge can be seen emanating from the anode.

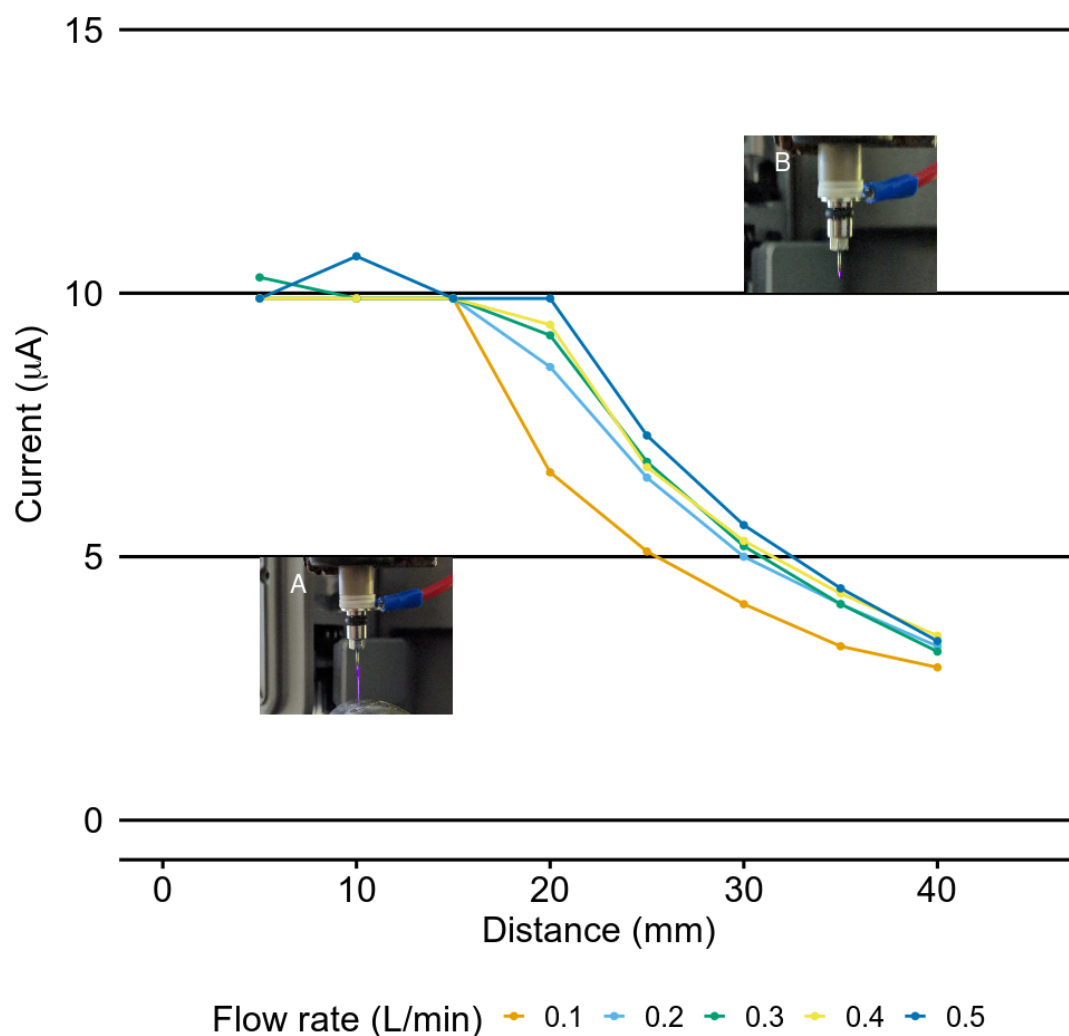


**Fig. 2.** Plot of current output between 5 and 40 mm at a range of gas flow rates with declining current observed above 20 mm. Photographs showing ignited ion source with the characteristic purple glow discharge of a helium plasma between the source anode (top) and counter electrode (bottom) at 5 mm electrode distance (**A**), and a photograph showing a much-shortened glow discharge at 40 mm electrode distance (**B**).

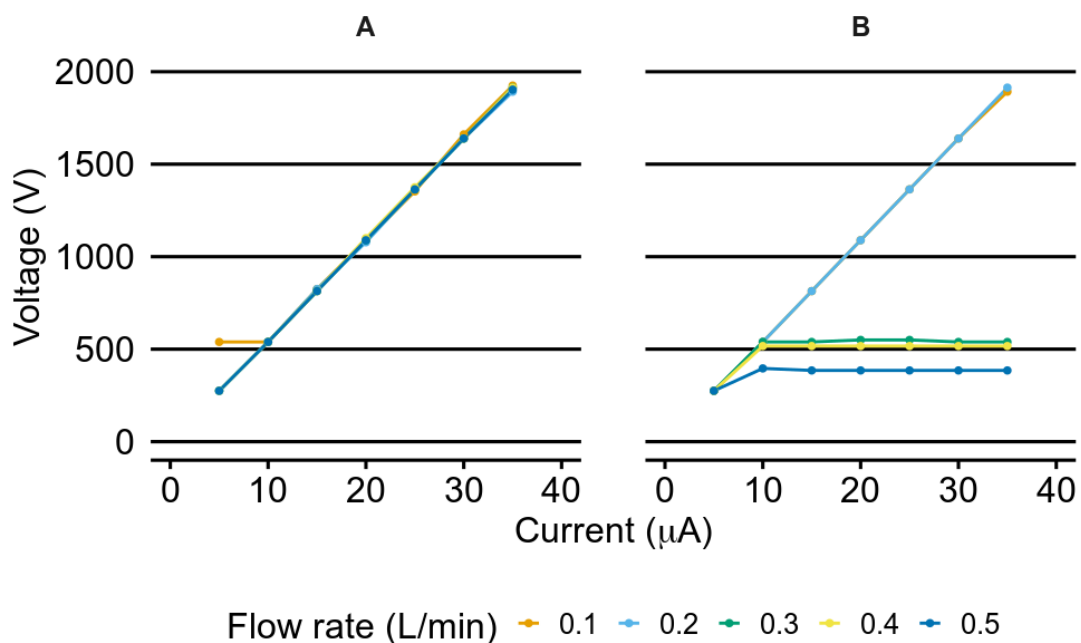


**Fig. 3.** Plot of current-voltage relationship at an electrode distance of 5 mm at five different flow rates showing a linear relationship, as would be expected in an abnormal glow discharge regime (**A**). Plot of current-voltage relationship at an electrode distance of 20 mm at five different flow rates, the linear relationship breaks down above 10  $\mu\text{A}$  and the voltage plateaux at flow rates of 0.3 to 0.5  $\text{L}\cdot\text{min}^{-1}$  (**B**).

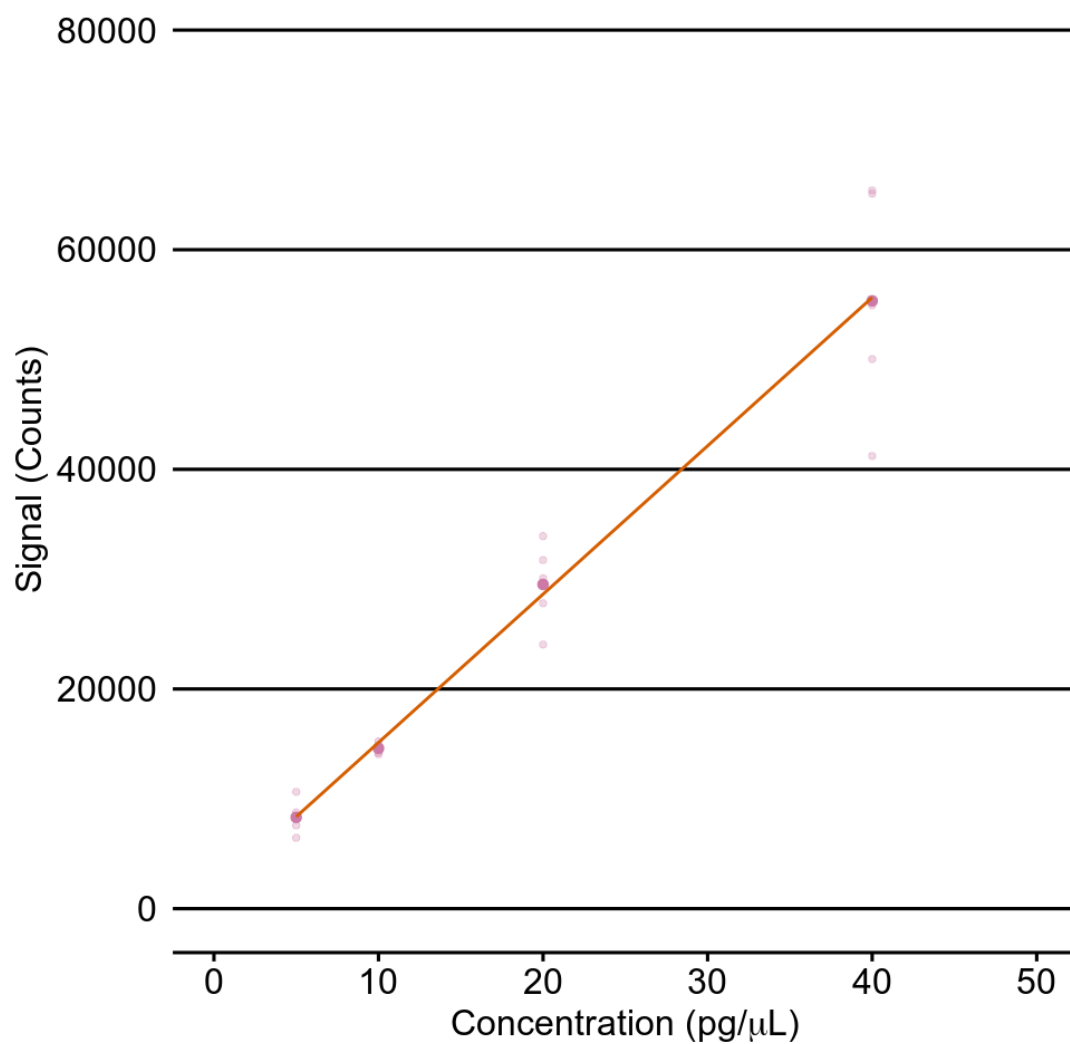


**Fig. 4.** Calibration plot showing the integrated signals of peak areas in full scan mode for methyl stearate ion at  $m/z$  299.29. Five replications at four different concentrations of methyl stearate (5, 10, 20, and 40  $\text{pg}\cdot\mu\text{L}^{-1}$ ) were introduced consecutively into the source (LOD = 111 fmol,  $N=5$ ,  $R^2 = 0.9991$ ).

Compound	Ionization Energy (eV)	Proton Affinity (kJ.mol <sup>-1</sup> )	Observed mass (% intensity)		
			Base peak	2nd	3rd
Bisphenol S (C <sub>12</sub> H <sub>10</sub> O <sub>4</sub> S)			251 [M+H]		
Bisphenol A (C <sub>15</sub> H <sub>16</sub> O <sub>2</sub> )			213 [M+H-O]	229.12 (10%)	243.14 (5%)
Pyrene (C <sub>16</sub> H <sub>10</sub> )	7.4	869.2	203 [M+H]	202.08 (80%)	219.08 (3%)
Anthracene (C <sub>14</sub> H <sub>10</sub> )	7.4	877.3	179 [M+H]	178.10 (70%)	
Octadecane (C <sub>18</sub> H <sub>38</sub> )			269 [M-H+O]	267.20 (40%)	
Dibenzofuran (C <sub>12</sub> H <sub>8</sub> O)			169 [M+H]	168.08 (80%)	185.08 (5%)
Tetradecane (C <sub>14</sub> H <sub>30</sub> )			213 [M-H+O]	211.17 (30%)	
Naphthalene (C <sub>10</sub> H <sub>8</sub> )	8.1	802.9	128 [M]	129 (95%)	145.08 (10%)
Dodecane (C <sub>12</sub> H <sub>26</sub> )			147 [M-23]	185.19 (90%)	
1,4-Dioxane (C <sub>4</sub> H <sub>8</sub> O <sub>2</sub> )	9.2	797.4	89 [M+H]		
Pentafluorobenzene (C <sub>6</sub> HF <sub>5</sub> )	9.6	690.4	167 [M]		
Hexafluoro-2-propanol (C <sub>3</sub> H <sub>2</sub> F <sub>6</sub> O)	12.2	686.6	167 [M]		
2,8-Dibromodibenzofuran (C <sub>12</sub> H <sub>6</sub> Br <sub>2</sub> O)			323 [M]		

**Table 1.** List of persistent organic pollutants and their analogues analysed using the Glow Flow helium-microplasma ion source and the ions observed in the resultant mass spectra. Proton affinities and ionization energies where listed are taken from [22, 23].

Compound	Repeating unit (Da)	Observed mass (% intensity)
Polyethylene glycol MW~400 Da	C <sub>2</sub> H <sub>4</sub> O 44	239.2 (50%), 283.2 (65%), 327.2 (70%), 371.2 (90%), 415.3 (100%), 459.3 (100%), 503.4 (65%), 547.4 (50%), 591.4 (20%)
Polypropylene glycol MW ~ 725 Da	C <sub>3</sub> H <sub>6</sub> O 58	483.4 (20%), 541.5 (45%), 599.5 (80%), 657.6 (100%), 715.6 (80%), 773.7 (55%), 831.7 (35%), 889.8 (20%), 947.8 (10%)
Polyethyleneimine	C <sub>2</sub> H <sub>5</sub> N 43	190.2 (30%), 233.3 (55%), 276.3 (100%), 319.4 (90%), 362.4 (50%), 405.5 (25%), 448.5 (20%)

**Table 2.** List of ions observed (with relative intensities, %) for the three polymers polyethylene glycol, polypropylene glycol and polyethyleneimine.

Common name	Formula	$M_r$	Observed ions
Methyl butyrate	C5H10O2	102.133	<i>n.o</i>
Methyl hexanoate	C7H14O2	130.187	<i>n.o</i>
Methyl octanoate	C9H18O2	158.241	<i>n.o</i>
Methyl decanoate	C11H22O2	186.295	<i>n.o</i>
Methyl laurate	C13H26O2	214.349	215.2
Methyl myristate	C15H30O2	242.403	243.2
Methyl palmitate	C17H34O2	270.457	271.3
Methyl stearate	C19H38O2	298.511	299.3
Methyl arachidate	C21H42O2	326.565	327.3
Methyl behenate	C23H46O2	354.619	355.3
Methyl lignocerate	C25H50O2	382.673	383.3

**Table 3.** List of the fatty acid methyl ester (FAME) compounds used as in the standard mixture for a single analysis, without any chromatographic separation, and corresponding  $m/z$  values for the ions observed using the helium-microplasma ion source between 50 and 350 °C.